HHS Public Access

Author manuscript

Int J Radiat Biol. Author manuscript; available in PMC 2015 October 01.

Published in final edited form as:

Int J Radiat Biol. 2014 October ; 90(10): 936–942. doi:10.3109/09553002.2014.922719.

Design and characterization of an economical ^{192}Ir hemi-brain small animal irradiator

Michael P. Grams[#], **Zachary C. Wilson**[#], **Terence T. Sio**, **Chris J. Beltran**, **Erik J. Tryggestad**, **Shiv K. Gupta**, **Charles R. Blackwell**, **Kevin P. McCollough**, **Jann N. Sarkaria**, and **Keith M. Furutani**

Department of Radiation Oncology , Mayo Clinic , Rochester , Minnesota , USA

[#] These authors contributed equally to this work.

Abstract

Purpose—To describe the design and dosimetric characterization of a simple and economical small animal irradiator.

Materials and methods—A high dose rate (HDR) ^{192}Ir brachytherapy source from a commercially available afterloader was used with a 1.3 cm thick tungsten collimator to provide sharp beam penumbra suitable for hemi-brain irradiation of mice. The unit was equipped with continuous gas anesthesia to allow robust animal immobilization. Dosimetric characterization of the device was performed with Gafchromic film measurements.

Results—The tungsten collimator provided a sharp penumbra suitable for hemi-brain irradiation, and dose rates on the order of 200 cGy/minute were achieved. The sharpness of the penumbra attainable with this device compares favorably to those measured experimentally for 6 MV photons, and 6 and 20 MeV electron beams from a linear accelerator, and was comparable to those measured for a 300 kVp orthovoltage beam and a Monte Carlo simulated 90 MeV proton beam.

Conclusions—Due to its simplicity and low cost, the apparatus described is an attractive alternative for small animal irradiation experiments requiring steep dose gradients.

Keywords

Small animal irradiator; hemi-brain; Iridium-192 HDR

Introduction

Small animal irradiation is an important part of radiation oncology research as it provides an opportunity to study the biologic and therapeutic effects of radiation on tumor and normal tissues. Complex small animal irradiation systems have been developed with associated treatment planning, multi-modality imaging, and precise positioning to allow irradiation of discrete regions within an experimental animal (Stojadinovic et al. 2007, Kiehl et al. 2008,

Correspondence: Dr Keith M. Furutani, Department of Radiation Oncology, Mayo Clinic, 200 First St SW, Rochester, MN 55905, USA. Tel: + 1 507 255 3806. furutani.keith@mayo.edu..

Declaration of interest

The authors report no conflicts of interest. The authors alone are responsible for the content and writing of the paper.

Wong et al. 2008, Verhaegen et al. 2011). However, the expense and availability of such systems may preclude many research groups from embarking on specific experiments. While the ability to image and accurately position the animal is necessary for the delivery of high-precision small animal radiotherapy, many informative experiments can be carried out with simple beam geometries and without complex imaging, positioning, and treatment planning capability. The purpose of this manuscript was to describe the design and characterization of a simple and economic small animal irradiator capable of hemi-brain irradiation in mice. The key criteria for the experimental device was a sharp penumbra that would minimize the dose of radiation delivered to the contralateral brain to provide an internal control in each mouse for irradiated versus unirradiated brain. The device uses a high dose rate (HDR) ^{192}Ir brachytherapy source from a commercially available afterloader and therefore is accessible to any radiation oncology department which offers HDR brachytherapy treatments in accordance with applicable national and state regulations.

Materials and methods

Photos of the apparatus are shown in Figure 1. The base plate for the apparatus that the mouse lies on is made from high strength, low thermal conductivity Delrin (polyoxymethylene) thermoplastic. A custom-made stainless steel bite block and a plastic nose cone for gas delivery/extraction were incorporated into the base plate to facilitate continuous animal gas anesthesia (Figure 2). The 0.9% iron, 2.1% nickel, 97% tungsten alloy collimator (Eagle Alloys Corporation, Talbott, TN, USA) is 4.8 × 4. 8 cm in dimension with a thickness of 1.3 cm and contains a 1.2 × 2.4 cm collimator opening. The collimator design allows the midline of the mouse to be visually aligned with the collimator edge for hemi-brain irradiation and threaded positioning pins allow for fine adjustment of the collimator after positioning the animal. A standard laboratory scissors jack allows for vertical positioning of the mouse on the Delrin platform such that the surface of the head is in contact with the bottom of the tungsten collimator. The collimator attaches to a 17.8 × 11.5 × 1.6 cm acrylic plate containing a groove for reproducible placement of the HDR catheter at the top surface of the collimator. When extended, the ^{192}Ir source is positioned at the center of the collimator opening and adjacent to the collimator edge as shown in Figure 1I. As described in the *Results* section, subsequent modifications of the collimator included use of a 1.3 cm thick acrylic insert to fill the opening and covering the bottom surface of the entire collimator with a film window.

Gafchromic film measurements were made to characterize the dose rate and penumbra of the collimator assembly. All film measurements were made with EBT3 Gafchromic film (Ashland ISP Advanced Materials, Bridgewater, NJ, USA) with film from the same lot (A04011302) and following the AAPM TG-55 recommendations for film handling (Niroomand-Rad et al. 1998). A nominal 6 MV linear accelerator was used to expose films to known doses in RMI 457 solid water (Gammex, Wisconsin, USA) to create a calibration curve and all subsequent film analysis was performed using FilmQA Pro® software (Ashland ISP Advanced Materials, Bridgewater, NJ, USA, version 3.0.4963.25489) using a one scan protocol (Lewis et al. 2012). Films were scanned in red-green-blue (RGB) format using a 48-bit scanner (Epson Expression 10000 XL) at 72 dpi, in transmission mode, and with no color or sharpness corrections. EBT3 film is energy independent down to energies

as low as 50 keV (Massillon-Jl 2012) and use in ^{192}Ir brachytherapy applications has been previously validated (Palmer et al. 2013). All film measurements were made at the surface as well as depths of 2 mm and 6 mm in a stack of RMI 457 solid water of 8 mm total thickness. RMI 457 solid water has been shown to be water equivalent for low energy photon beams down to 50 kVp (Hill et al. 2010). A VariSource iX afterloader (Varian Medical Systems, Palo Alto, CA, USA) extended the ^{192}Ir HDR source such that the center of the active length was placed at the midpoint of the collimator opening immediately adjacent to its edge. A dwell time of 1 min was used to expose all films. Dose rates are defined in units of cGy/min/Ci to incorporate the source activity.

The penumbra from the ^{192}Ir small animal irradiator was compared under similar small field collimating conditions to the penumbra from 6 MV photons, 6 MeV electrons, and 20 MeV electrons from a Varian 21EX linear accelerator (Varian Medical Systems, Palo Alto, CA, USA) as well as 300 kVp photons from an orthovoltage unit (Maxitron 300, General Electric, Milwaukee, WI, USA) and Monte Carlo simulated 90 MeV protons. Measurements with the linear accelerator were taken at 100 cm source to surface distance using the 8 mm thick solid water stack with films positioned at 2 mm and 6 mm depth. The 6 MV data was acquired with one jaw closed along the central axis of the beam providing a half-beam block geometry and the overall field size was 1.2 × 2.4 cm. The 6 MeV and 20 MeV electron data were acquired with the same linear accelerator using a 10 × 10 cm cone and the tungsten collimator placed on the surface of the solid water stack to define the collimated field size. The orthovoltage results were obtained using a 300 kVp beam with a 2 mm copper filter, a source to surface distance of 60 cm, and films placed at 2 mm and 6 mm depth in the 8 mm solid water stack with the tungsten collimator placed on the surface to define the field size. Monte Carlo simulation was employed to derive the dosimetric characteristics of the tungsten collimator. The 90 MeV beam characteristics were simulated using TOPAS/GEANT4 (Agostinelli et al. 2003, Perl et al. 2012) and based upon the proton spot scanning facility currently under construction at our institution. The proton spot size (1-sigma) at 90 MeV is 4 mm, and the collimator was placed at isocenter of the treatment machine. At this energy the protons that impinge on the tungsten collimator fully stop. A 4 × 4 cm field size with a 4 mm spot spacing was used for the simulation and the spot weights were adjusted to provide a uniform dose transverse to the beam at the depth of interest in the absence of the tungsten collimator.

A hemi-brain irradiation study was carried out with the apparatus to demonstrate the potential for sparing of the contralateral brain hemisphere. The total time to set up the apparatus, including anesthesia, was approximately 15 min. All animal studies were reviewed and approved by the Mayo Institutional Animal Use and Care Committee. Mice were irradiated to the hemi-brain with a single fraction of 2 Gy under continuous gas anesthesia. Oxygen gas mixed with 2–3% isoflurane was delivered at a rate of 1–2 l/min through the central part of the nose cone and withdrawn through a surrounding vacuum extraction port. Mice were euthanized by CO_2 inhalation 30 min after irradiation and immediately perfused with ice cold saline followed by 4% paraformaldehyde. The brain was removed, immersed in 4% paraformaldehyde/10% sucrose overnight at 4°C, and then cryopreserved in optimal cutting temperature (Torrance, CA, USA) and processed for sectioning. After antigen retrieval in 10 mM sodium citrate buffer at 80°C for 1 h, slides

were washed with phosphate buffer saline (PBS) and blocked with 5% goat serum at room temperature for 1 h before applying biotin labeled anti-human monoclonal antibody to γH2AX clone JBW301 (Millipore, Temecula, CA, cat #16-193) diluted 1/500 in 5% goat serum, and incubated at 4°C overnight. Slides were then rinsed 3 times with PBS and incubated with Alexa Fluor-488 conjugated streptavidin (Invitrogen, Eugene, OR, USA) at room temperature for 1 h, washed with PBS and mounted with Slowfade containing DAPI (Invitrogen, Eugene, OR). Immunostained brain sections were visualized on a fluorescence microscope (Leica AF6000, Mannheim, Germany) equipped with an automated stage and camera. Tiled images were obtained with a 5 × objective.

Results

Collimator design

The choice of collimator material was driven by the desire for a maximum dose rate while still adequately sparing the contralateral brain. Due to its availability and low cost, the initial collimator design used lead of 1.9 cm thickness, and a dose rate of 15 cGy/min/Ci at 2 mm depth was obtained with acceptable penumbra and shielding. Although a more expensive material, a much higher dose rate of 25 cGy/min/ Ci at 2 mm depth was obtained using a 1.3 cm thick tungsten collimator without compromising the penumbra or overall shielding. Following the inverse square law, the higher dose rate with the tungsten collimator is mainly due to the 6 mm reduction in distance from the source. For HDR brachytherapy units having activities between 4 and 10 Ci, dose rates of 100–250 cGy/min at 2 mm depth are attainable with this collimator.

Initial film measurements identified prohibitively high surface doses from low energy electrons ejected from the sides of the collimator opening. These electrons deliver dose only at very shallow depths and are easily attenuated. A partial solution to the problem of high surface dose was obtained by filling the entire collimator opening with a water equivalent acrylic insert (Figure 1H) which attaches directly to the acrylic plate (Figure 1D). This reduced the surface dose rate throughout most of the field from approximately 120 cGy/min/Ci to 30 cGy/min/Ci (Figure 3A and B). However, high surface doses remained at the periphery of the collimator opening due to the presence of small air gaps between the collimator and the acrylic insert from the inevitable imperfections in machining (Figure 3B). To eliminate these peripheral hotspots, a window consisting of a single piece of Gafchromic film (0.28 mm thickness) was used to completely cover the bottom of the collimator opening. In conjunction with the acrylic collimator insert, this approach provided a highly uniform surface dose without the presence of hotspots (Figure 3C and D). Similar measurements were made at 2 mm and 6 mm depths with or without the acrylic insert and/or the film window. As seen in Table I, the combination of the acrylic insert and film window was most effective at eliminating the high surface dose without significantly affecting the dose rate at depth.

Penumbra and beam characterization

The uniformity of dose across the collimator opening was evaluated for the final tungsten collimator design with the acrylic insert and film window in place. Figure 4 shows dose

profiles at 2 mm depth for transverse (4A) and longitudinal (4B) directions for the tungsten collimator with the ^{192}Ir source. The dose profile in the transverse direction demonstrates a very sharp penumbra with the dose increasing from 20–80% of maximum over a distance of 0.7 mm (Table II). The profiles in Figure 4 indicate a relatively uniform dose is delivered over 5 mm in the transverse direction and 10 mm in the longitudinal direction. This region of uniformity encompasses a typical mouse hemi-brain, which measures approximately 5–7 mm (transverse) by 8–12 mm (longitudinal) by 5–7 mm (depth). While the dose is uniform within the target at depth, the dose delivered will decrease with increasing distance from the brachytherapy source. Such a dose profile provides a unique opportunity to evaluate the impact of graded doses of radiation across a brain specimen with excellent sparing of the contra-lateral hemisphere. To demonstrate this concept, mice were irradiated with 2 Gy to the hemi-brain and then euthanized 30 min later and processed for γH2AX staining as a measure of DNA damage induction. Consistent with the dosimetric evaluations, robust γH2AX staining was observed in the irradiated but not the unirradiated hemisphere as seen in the coronal image of a mouse brain (Figure 5).

Penumbra comparisons

Direct comparison of the penumbra at 2 mm and 6 mm depths from the ^{192}Ir small animal irradiator to other delivery modalities is shown in Figures 6 and 7. The data has been normalized to the maximum dose and rescaled such that the zero position corresponds to the 50% dose point of each individual modality. Figure 6 compares the ^{192}Ir small animal irradiator to modalities universally available in all radiation oncology departments, namely, megavoltage photon and electron beams. As anticipated, the penumbra for the photon beam is relatively broad with an increase from 20–80% of maximum occurring over 2 mm and 2.5 mm at depths of 2 mm and 6 mm, respectively. For the electron beams, 6 MeV electrons had a sharp penumbra at 2 mm depth (1.1 mm) but the penumbra was less sharp at 6 mm depth (2.8 mm). In contrast, the 20 MeV beam maintained a sharp penumbra similar to the ^{192}Ir beam at both 2 mm and 6 mm depths (0.8 and 1.2 mm, respectively), but the dose underneath the collimator was 8–9% of maximum due to bremsstrahlung radiation originating within the tungsten. Thus, for the common clinically available radiation sources, ^{192}Ir provides the sharpest penumbra for optimal sparing of the contralateral hemisphere.

Figure 7 compares the ^{192}Ir small animal irradiator to the 300 kVp orthovoltage unit and a 90 MeV proton beam, which represent modalities less common in typical radiation oncology centers. The penumbra for the orthovoltage beam was quite sharp with dose increasing from 20–80% of maximum across 0.5 mm and 0.6 mm at 2 mm and 6 mm depths, respectively. Due to the inherent lower energy, dose under the tungsten collimator was less for 300 kVp photons as compared to ^{192}Ir. The Monte Carlo calculated profile for the 90 MeV proton beam demonstrated the sharpest penumbra (0.2 mm) with significantly less dose under the collimator. Thus, orthovoltage and proton beams provide superior penumbra and shielding characteristics as compared to the ^{192}Ir small animal irradiator.

Discussion

The availability of a convenient and economical radiation source can limit the capacity to perform animal experiments in many academic centers. Orthovoltage radiation units and proton beams offer exceptionally sharp penumbra and relatively uniform dose distributions, but are not as commonly available as linear accelerators and HDR brachytherapy afterloaders, which are almost universal in radiation oncology clinical facilities. Both megavoltage electron and photon beams from linear accelerators can be used for animal irradiation, but as demonstrated here, the penumbra is much broader for these beams and may limit their utility in applications where a steep dose gradient is required. In contrast, the ^{192}Ir small animal irradiator provides a penumbra that is comparable to orthovoltage beams but it is limited to irradiating from one direction and therefore cannot provide uniform dose to the entire depth of the brain. A more uniform dose distribution could be obtained using a larger source to target distance at the expense of a significantly reduced dose rate. Alternatively, the irradiator design described here could easily be extended to a dual transit tube, dual collimator design to provide irradiation from opposing sides of the animal (Stojadinovic et al. 2007).

High surface doses initially posed a significant challenge to implementation of the small animal irradiator. As the data in Table I shows, the surface dose is more than 4 times the dose at 2 mm depth without an acrylic insert and/or film window. Thus, without attenuation of the surface dose, total doses for a single fraction dose at 2 mm depth would be limited to approximately 4–5 Gy; in a pilot study, one mouse developed a severe skin reaction two weeks after being exposed to a surface dose of 20 Gy. Several other authors have reported similarly high surface doses when using metallic collimating devices for orthovoltage radiotherapy (Podgorsak, 1990, Lye et al. 2010, Arndt et al. 2011). The acrylic insert within the collimator reduced the surface dose without significantly reducing the dose rate at depth since the inherent attenuation is partially offset by the increased dose due to scatter within the acrylic. However, regions of high dose remained around the periphery of the collimator opening due to small gaps between the insert and the tungsten. While placement of the film window at the bottom of the collimator opening provided an immediate and convenient solution, the film precludes visual alignment of the mouse. A similar thickness of clear plastic provides comparable results while still allowing for convenient visual alignment.

Conclusion

The small animal irradiator described in this paper has several characteristics which make it an attractive option for small animal irradiation experiments. The apparatus can be built for under $ 1,000 and used in conjunction with any commercial brachytherapy afterloader to provide a convenient and cost-effective option for small animal irradiation experiments. The unit offers high dose rate delivery and sharp penumbra, which is ideal for hemi-brain irradiation of mice. With slight modifications to the design, irradiation of sites other than the brain could be accomplished easily. Additionally, scheduling animal irradiation on a HDR brachytherapy unit could be more convenient in a busy clinical department since HDR after-loaders are used intermittently as compared to almost constant use of linear accelerators during working hours. In the event other modalities are unavailable or impractical, the ^{192}Ir

small animal irradiator could be an effective and convenient alternative for small animal irradiation research.

References

Agostinelli S, Allison J, Amako K, Apostolakis J, Araujo H, Arce P, Asai M, Axen D, Banerjee S, et al. GEANT4-a simulation toolkit. Nuc Instrum Meth Phys Res A: Accelerat Spectrom Detect Assoc Equip. 2003; 506:250–303.

Arndt CD, Wang IZ, Saito NG, Podgorsak MB. Dosimetric calibration and characterization for experimental mouse thoracic irradiation using orthovoltage X rays. Radiat Res. 2011; 175:784–789. [PubMed: 21449715]

Hill R, Kuncic Z, Baldock C. The water equivalence of solid phantoms for low energy photon beams. Medical Phys. 2010; 37:4355.

Kiehl EL, Stojadinovic S, Malinowski KT, Limbrick D, Jost SC, Garbow JR, Rubin JB, Deasy JO, Khullar D, Izaguirre EW, Parikh PJ, Low DA, Hope AJ. Feasibility of small animal cranial irradiation with the microRT system. Med Phys. 2008; 35:4735. [PubMed: 18975718]

Lewis D, Micke A, Yu X, Chan MF. An efficient protocol for radiochromic film dosimetry combining calibration and measurement in a single scan. Med Phys. 2012; 39:6339–6350. [PubMed: 23039670]

Lye JE, Butler DJ, Webb DV. Enhanced epidermal dose caused by localized electron contamination from lead cutouts used in kilovoltage radiotherapy. Med Phys. 2010; 37:3935. [PubMed: 20879556]

Massillon-JL G. Energy dependence of the new Gafchromic EBT3 film:dose response curves for 50 KV, 6 and 15 MV X-ray beams. Int J Med Phys, Clin Engineer Radiat Oncol. 2012; 1:60–65.

Niroomand-Rad A, Blackwell CR, Coursey BM, Gall KP, Galvin JM, McLaughlin WL, Meigooni AS, Nath R, Rodgers JE, Soares CG. Radiochromic film dosimetry: Recommendations of AAPM Radiation Therapy Committee Task Group 55. Med Phys. 1998; 25:2093–2115. [PubMed: 9829234]

Palmer AL, Di Pietro P, Alobaidli S, Issa F, Doran S, Bradley D, Nisbet A. Comparison of methods for the measurement of radiation dose distributions in high dose rate (HDR) brachytherapy: Ge-doped optical fiber, EBT3 Gafchromic film, and PRESAGE(R) radiochromic plastic. Med Phys. 2013; 40:061707. [PubMed: 23718586]

Perl J, Shin J, Schumann J, Faddegon B, Paganetti H. TOPAS: An innovative proton Monte Carlo platform for research and clinical applications. Med Phys. 2012; 39:6818–6837. [PubMed: 23127075]

Podgorsak MB. Surface dose in intracavitary orthovoltage radiotherapy. Med Phys. 1990; 17:635. [PubMed: 2215408]

Stojadinovic S, Low DA, Hope AJ, Vicic M, Deasy JO, Cui J, Khullar D, Parikh PJ, Malinowski KT, Izaguirre EW, Mutic S, Grigsby PW. MicroRT – Small animal conformal irradiator. Med Phys. 2007; 34:4706. [PubMed: 18196798]

Verhaegen F, Granton P, Tryggestad E. Small animal radiotherapy research platforms. Phys Med Biol. 2011; 56:R55–83. [PubMed: 21617291]

Wong J, Armour E, Kazanzides P, Iordachita I, Tryggestad E, Deng H, Matinfar M, Kennedy C, Liu Z, Chan T, Gray O, Verhaegen F, McNutt T, Ford E, Deweese TL. High-resolution, small animal radiation research platform with X-ray tomographic guidance capabilities. Int J Radiat Oncol, Biol, Phys. 2008; 71:1591–1599. [PubMed: 18640502]

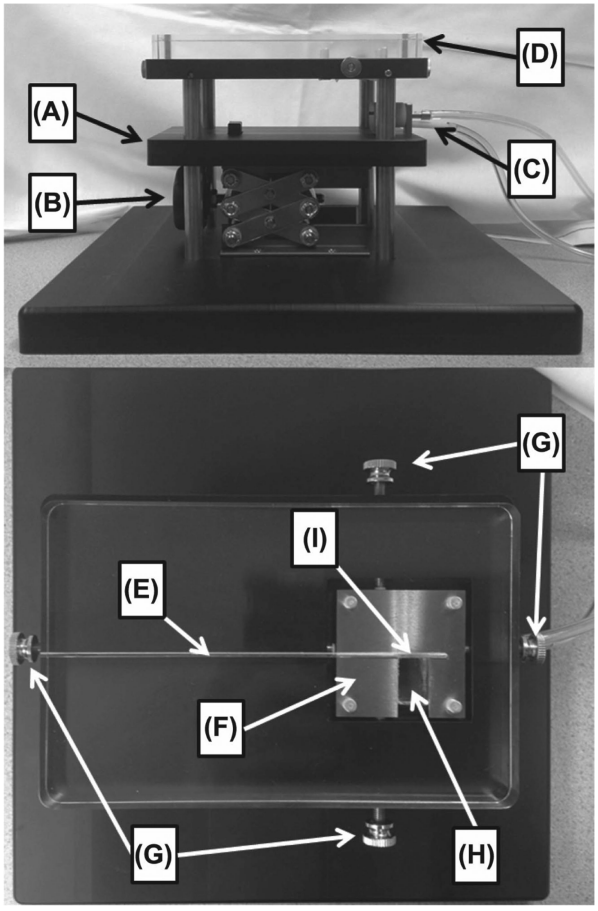

Figure 1.

Photos of the small animal irradiator. (A) Delrin platform; (B) Laboratory scissors jack; (C) Gas delivery/extraction system; (D) Acrylic plate for guiding the HDR catheter; (E) HDR catheter guide; (F) Tungsten collimator; (G) Collimator positioning pins; (H) Acrylic collimator insert; (I) Location of ^{192}Ir source when extended.

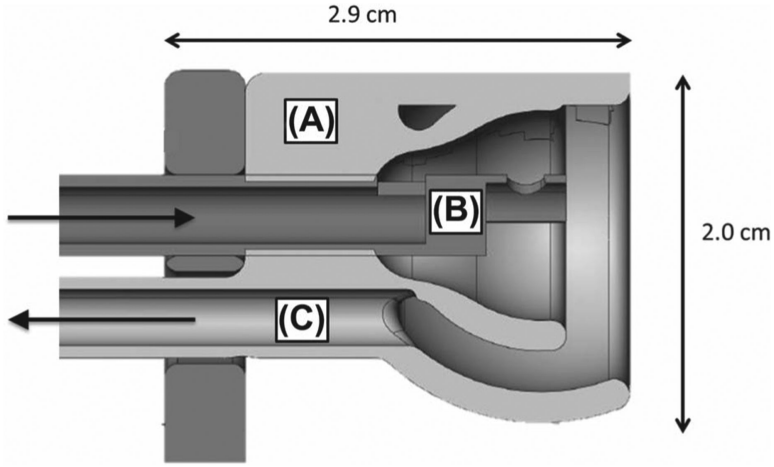

Figure 2.

Nose cone and gas delivery assembly. (A) Plastic nose cone; (B) Stainless steel bite block and gas delivery tube; (C) Vacuum extraction port.

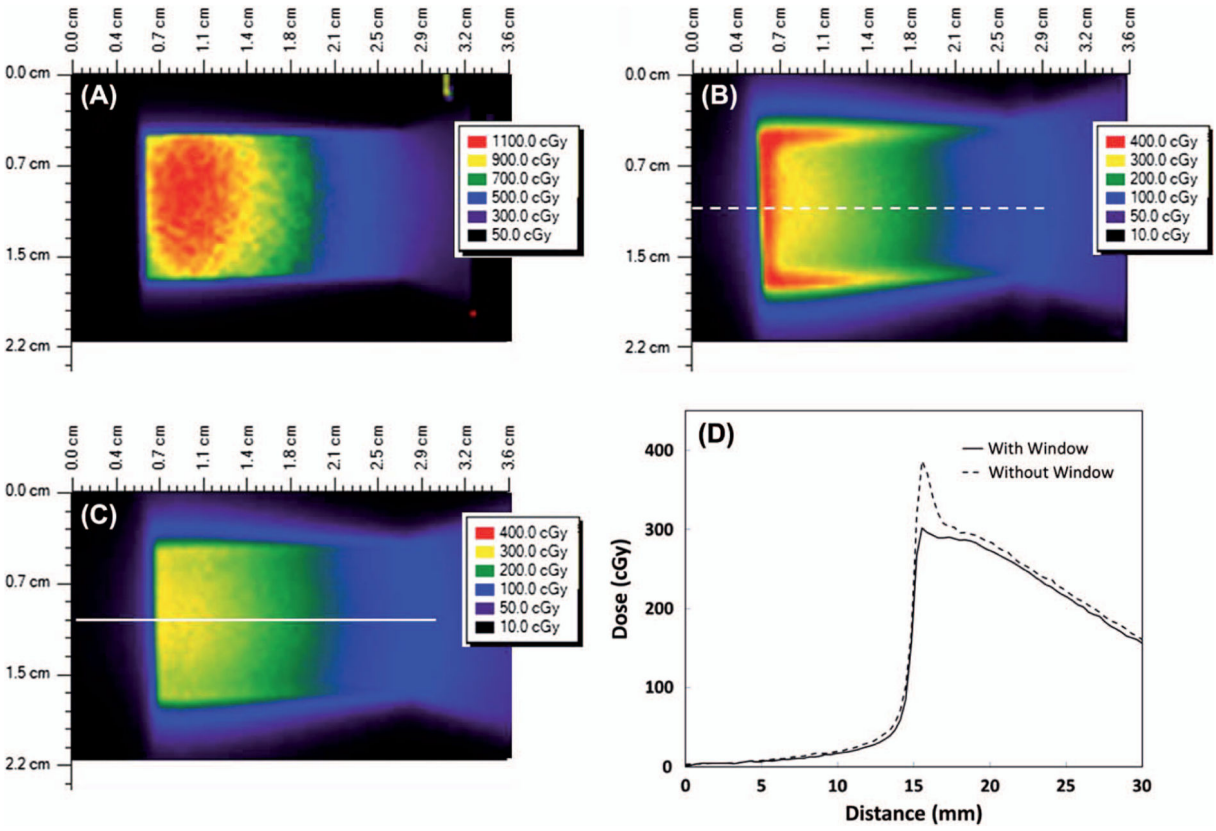

Figure 3.

Color wash depictions of the surface dose under various collimator design scenarios using the ^{192}Ir source. Note the different dose scale in Figure A. All measurements were made with an exposure time of 1 minute using an 8.9 Ci source. The dashed and solid lines in B and C indicate the location of the corresponding dose profiles shown in D. (A) Open collimator without film window; (B) Collimator with water equivalent insert in place, but without the film window; (C) Collimator with water equivalent insert in place, and with film window covering the bottom of the collimator; (D) Dose profiles at locations indicated by dashed and solid lines in B and C for the collimator with the water equivalent window in place, both with and without the film window. This Figure is reproduced in color in the online version of the *International Journal of Radiation Biology* .

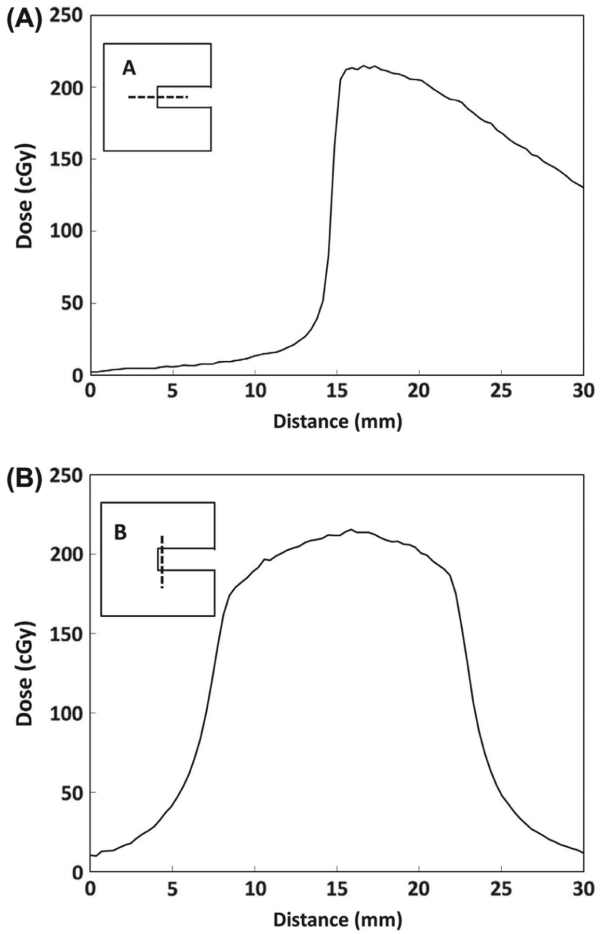

Figure 4.

Dose profiles for the transverse (A) and longitudinal (B) directions at 2 mm depth using the tungsten collimator and the ^{192}Ir source. The inset shows the outline of the collimator and the dashed lines indicate the location of the dose profiles relative to the collimator opening. The exposure time was 1 minute with an 8.9 Ci source.

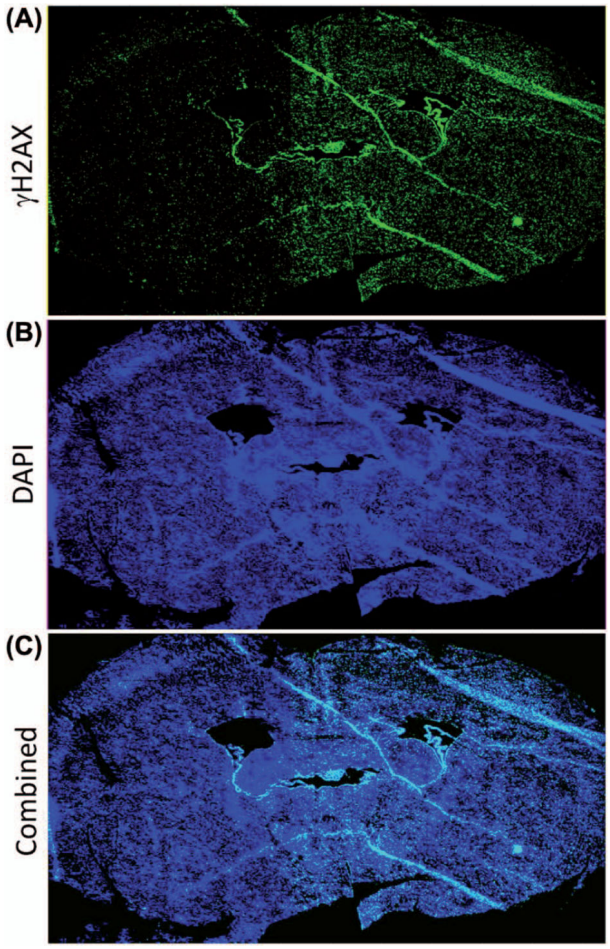

Figure 5.

γH2AX stained image of a coronal slice of mouse brain irradiated to 2 Gy using the ^{192}Ir hemi-brain small animal irradiator. (A) Bright green regions corresponding to locations of increased DNA double-strand breaks are visible on the right side of the image which was the irradiated half of the brain; (B) Bright blue regions represent 4′,6-diamidino-2-phenylindole (DAPI) fluorescent crosslinking with DNA which marked the location of fixed cells within parenchyma of the stained mouse brain; (C) A combined image of the γH2AX and DAPI stains above. This Figure is reproduced in color in the online version of the *International Journal of Radiation Biology*.

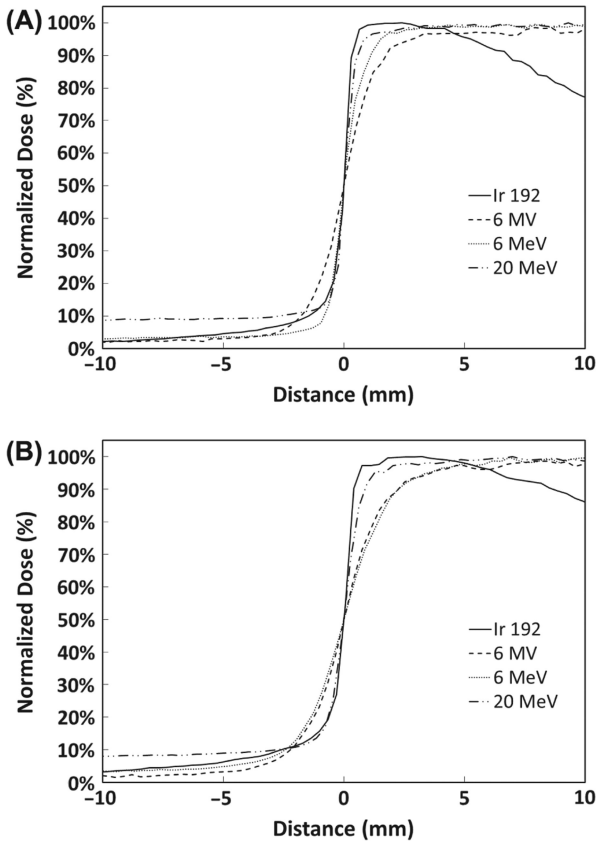

Figure 6.

Transverse penumbra at 2 mm (A) and 6 mm (B) depth for the ^{192}Ir small animal irradiator, 6 MV photon, and 6 and 20 MeV electron beams.

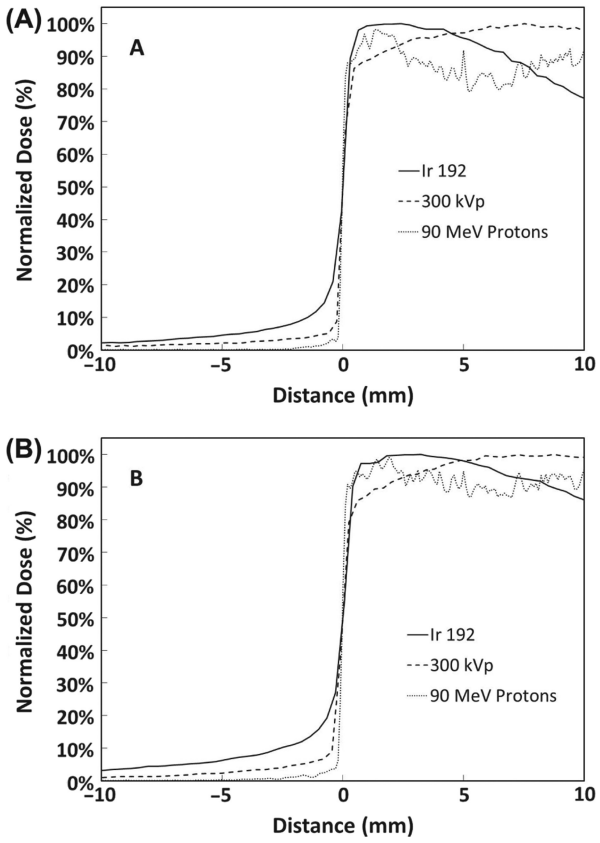

Figure 7.

Transverse penumbra at 2 mm (A) and 6 mm (B) depth for the ^{192}Ir small animal irradiator, 300 kVp orthovoltage unit, and 90 MeV proton beam.

Table I

Maximum dose rates measured at the surface, 2 mm depth, and 6 mm depth. Measurements were made with and without the acrylic insert in place, and also with and without the additional film window.

Dose rates at various depths				
Maximum dose rate (cGy/min/Ci)	**Without acrylic collimator Insert**		**With acrylic collimator Insert**	
Depth	**Window**	**No window**	**Window**	**No window**
Surface	54	121	33	43
2 mm depth	27	28	24	25
6 mm depth	16	17	14	15

Table II

Distance (in mm) between 20% and 80% of the maximum dose measured in the penumbral region for various modalities measured at 2 mm and 6 mm depth.

	20-80% penumbra distance in millimeters					
Depth	**Ir 192 Photons**	**6 MeV Electrons**	**20 MeV Electrons**	**6 MV Photons**	**300 kVp Photons**	**90 MeV Protons**
2 mm	0.7	1.1	0.8	2	0.5	0.2
6 mm	0.9	2.8	1.2	2.5	0.6	0.2